

Internal friction study of the phase transition in $\text{GdBaCo}_2\text{O}_{5+\delta}$ bulk materials

X. S. Wu, H. L. Zhang, J. R. Su, C. S. Chen, and W. Liu*

Laboratory of Advanced Functional Materials and Devices, Department of Materials Science and Engineering, University of Science and Technology of China, Hefei 230026, People's Republic of China

(Received 10 February 2007; revised manuscript received 29 June 2007; published 11 September 2007)

The internal friction and shear modulus at low frequency together with the electrical and magnetic properties have been measured for an ordered oxygen-deficient perovskite $\text{GdBaCo}_2\text{O}_{5+\delta}$ ceramics ($\delta=0.005, 0.499, \text{ and } 0.515$). For $\delta=0.005$, an internal friction peak at 225 K and the corresponding softening of shear modulus were observed, showing the existence of lattice distortion. This lattice distortion indicates the presence of charge ordering, which conforms to the slight upturn on the electrical resistivity curve. The anomalies in shear modulus and the internal friction peak at about T_{CO} were suggested to be correlated with the structure change caused by the Jahn-Teller effect of Co^{3+} (HS state) located in square pyramidal sites. For $\delta=0.499$ and 0.515, a large softening of shear modulus accompanied by an increasing of internal friction was observed at low temperature, which is related to the antiferromagnetic-ferromagnetic transition. And the internal friction peak with the features of phase transition at about 350 K can be ascribed the metal-insulator transition. At high temperature, the relaxation internal friction peak accompanied by the corresponding decrease of shear modulus originates from the oxygen hopping in $[\text{GdO}_\delta]$ planes.

DOI: 10.1103/PhysRevB.76.094106

PACS number(s): 62.40.+i, 75.47.Pq, 71.38.-k, 75.30.Kz

I. INTRODUCTION

Transition metal oxides with perovskite structure have attracted considerable attention because of their fascinating physical properties such as colossal magnetoresistance (MR) in manganese and high- T_c superconductivity in copper oxides. A great many experimental and theoretical efforts have been made to clarify the nature of these physical properties. Recently the ordered oxygen-deficient perovskites, of general description $\text{RBA}\text{Co}_2\text{O}_{5+\delta}$ ($R=\text{lanthanide}, 0 \leq \delta \leq 1$), have attracted much interest as a spin-charge-orbital coupled system.¹⁻¹² The crystal structure is derived from the “112” structure of YBaCuFeO_5 (Ref. 13) and is formed from the stacking sequence of $[\text{CoO}_2]$ - $[\text{BaO}]$ - $[\text{CoO}_2]$ - $[\text{RO}_\delta]$ along the c direction. In the case of $\delta=0$, all the Co ions are located within square pyramids with a fivefold coordination. With the increase of oxygen content δ , a part of Co ions have an octahedral environment. In the special case of $\delta=0.5$ only Co^{3+} is expected, oxygen ions and oxygen vacancies are located in alternating rows within the $[\text{RO}_\delta]$ planes, which result in an alternating rows of square-pyramidal and octahedral Co^{3+} sites.^{2,6} For $\delta=1$, the cobalt environment appears to be exclusively octahedral.

The oxygen content δ controls not only the crystal structure but also physical properties of these oxides. For instance, samples with $\delta=0$ present a charge ordering of $\text{Co}^{2+}/\text{Co}^{3+}$ ions (at least for $R=\text{Y},^3 \text{ Ho},^4,5 \text{ Tb},^5 \text{ and Dy}^5$) at low temperature ($T_{\text{CO}}=220$ K for $R=\text{Y}$), which is accompanied by a strong enhancement in the splitting of the a and b axes. However, the charge ordering was not observed in the $\text{YBaCo}_2\text{O}_{5+\delta}$ samples with the oxygen content δ slightly in excess of zero.³ Furthermore, samples with $\delta=0$ mentioned above undergo a paramagnetic (PM) to antiferromagnetic (AFM, G -type) transition at T_N ($T_N=330$ K for $R=\text{Y}$) together with a tetragonal to orthorhombic structure phase transition.³⁻⁵ Although a lot of experimental and theoretical work has been done, there is still some controversy about the

spin states of Co ions in the $\text{RBA}\text{Co}_2\text{O}_5$.^{3-5,14-16} The compounds with $\delta \approx 0.5$ present a metal-insulator (MI) transition at $T_{\text{MI}} \approx 280-400$ K depending on the rare earth R ,² and this transition is usually associated to a spin-state change of the Co^{3+} ion on the octahedral site.^{1,2,10,11} Moreover, it is commonly observed in these compounds with successive PM-FM-AFM transitions.^{1,2,6,11} Several different models have been proposed to explain the narrow temperature region of FM order and the subsequent FM-AFM transition upon cooling.^{6-8,11} One of them developed by Moritomo *et al.* suggests that the competition between an inherent AFM superexchange interaction and a FM double-exchange interaction due to carrier localization was the origin for the FM and FM-AFM transition.⁶

The internal friction technique is a very sensitive tool in studying microscopic relaxation processes and structure phase transitions in solid materials.¹⁷⁻²¹ In this paper, we present the results of the internal friction investigation of $\text{GdBaCo}_2\text{O}_{5+\delta}$ oxide. Combined with the results of magnetic and electrical measurements, it is found that some features of internal friction and shear modulus can be correlated well with the magnetic phase transitions and/or carrier transportation alternations.

II. EXPERIMENT

The rectangular ceramics samples in form of $30 \times 4.2 \times 1.5$ mm³ are prepared by the conventional solid state reaction. Stoichiometric mixture of Gd_2O_3 , BaCO_3 , and Co_2O_3 was ground and calcined in air at 950, 1000, 1050 °C for 10 h, respectively. The product was then reground, palletized, and sintered at 1100 °C for 20 h in air. The purity of the compound was checked by x-ray diffraction at room temperature by using a Philips diffractometer with CuK_α radiation. The oxygen content δ was adjusted by changing temperature and atmosphere of subsequent annealing, and was determined by iodometric titration. For each sample, the ti-

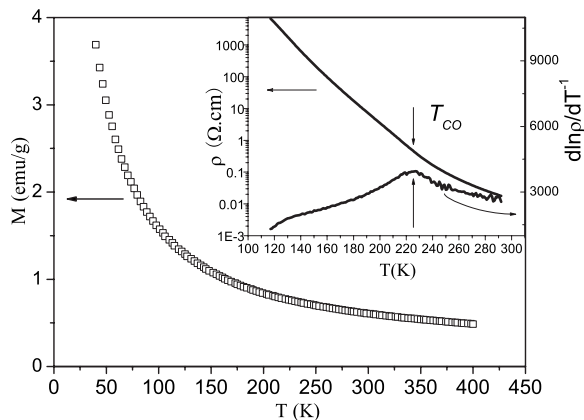


FIG. 1. The variation of the magnetization [$M(T)$] for $\text{GdBaCo}_2\text{O}_{5.005}$ in a field of 1 T as a function of the temperature (zero-field cooled and taken on heating). The inset shows variations of the resistivity ρ and the logarithmic derivative $d(\ln \rho)/dT^{-1}$, of the resistivity with temperature for $\text{GdBaCo}_2\text{O}_{5.005}$.

tration was repeated for 3–5 times. The resistivity was measured by the standard four-probe technique. The magnetization and ac susceptibility were measured using a commercial quantum device (ac-dc superconducting quantum interference device; Quantum Design MPMSXL). The internal friction Q^{-1} and shear modulus G were measured in a computer-controlled automatic inverted torsion pendulum with the forced-vibration method with the maximum torsion strain amplitude kept at 1.5×10^{-5} . The dynamic modulus was expressed according to the relation $G^* = G \exp(i\varphi) = G' - iG''$, φ is the lag angle between the stress imposed and the resulting strain. The mechanical losses versus temperature $Q^{-1}(T)$ were given by the ratio G''/G' and the shear modulus $G(T)$ was equal to G' .

III. RESULTS AND DISCUSSION

The excess oxygen content δ of investigated samples is determined to be 0.005, 0.499, and 0.515. The x-ray diffraction data at room temperature show that the peaks of samples with $\delta=0.499$ and 0.515 can be indexed with orthorhombic symmetry with a space group $Pmmm$, while the sample of $\delta=0.005$ keeps (a macroscopically tetragonal) with a space group $P4/mmm$.

The variation of the magnetization [$M(T)$] of $\text{GdBaCo}_2\text{O}_{5.005}$ in a field of 1 T as a function of the temperature measured after a zero-field cooling (ZFC) process is shown in Fig. 1. It can be seen that the compound exhibits a typical paramagnetic (PM) behavior in the temperature range of 40–400 K. The indications of the charge ordered state and antiferromagnetic (AFM) ordered state observed in the isostructural YBaCo_2O_5 (Ref. 3) are not detected from the $M(T)$ curve of $\text{GdBaCo}_2\text{O}_{5.005}$. However, one can see from the inset in Fig. 1, there is a slight upturn at about 225 K in the $\rho(T)$ curve, which means the $\text{Co}^{2+}/\text{Co}^{3+}$ charge ordered state may still exist in $\text{GdBaCo}_2\text{O}_{5.005}$. Besides variation of resistivity at the T_{CO} , there are generally changes of crystal parameters accompanied by the charge ordering.²² In fact, a

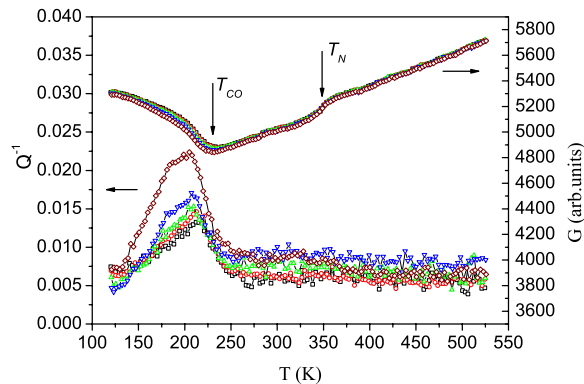


FIG. 2. (Color online) Temperature dependence of the shear modulus and internal friction of $\text{GdBaCo}_2\text{O}_{5.005}$ with various frequencies at a heating rate of 2 K/min.

strong enhancement in the splitting of the a and b axes have been observed in YBaCo_2O_5 (Ref. 3) and $\text{HoBaCo}_2\text{O}_5$,^{4,5} respectively, at the T_{CO} . We speculate that the lattice distortion should exist in $\text{GdBaCo}_2\text{O}_5$ near T_{CO} , too.

Considering that the modulus softening, caused by the lattice distortion, can be sensitively detected by the internal friction method, we carry out a study of shear modulus G and internal friction Q^{-1} of $\text{GdBaCo}_2\text{O}_{5.005}$ with various frequencies. The experimental results are given in Fig. 2, and we can see that with increasing temperature, the shear modulus softens and reaches a minimum at about T_{CO} . After passing through the minimum, the modulus begins to increase with further increasing temperature. The softening of the modulus, which exhibits essential signatures of a phase transition, indicates a drastic instability of the lattice near T_{CO} . That is to say, the electron-lattice coupling may play an important role in the CO phase transition. A similar remarkable change of shear modulus in the vicinity of T_{CO} was also reported in manganite oxides.^{20,21} There, the elastic softening has been suggested to originate from the coupling of the orbital moment of e_g of Mn^{3+} ion to the elastic strain. Similarly, our results can be explained as the coupling between the lattice strain and the charges via the Jahn-Teller effect of Co^{3+} ions. In fact, this Jahn-Teller active high spin Co^{3+} ions (t_{2g} electron) in YBaCo_2O_5 , which favor the stripe-type $\text{Co}^{2+}/\text{Co}^{3+}$ charge ordering, were strongly suggested by Wang *et al.* based on their theoretical calculation results.¹⁵ This suggestion further make us believe that Co^{3+} ions in $\text{GdBaCo}_2\text{O}_{5.005}$ should be in a high spin state for realizing the coupling between electron and phonon. From Fig. 2, a wide and asymmetrical internal friction peak was observed during the CO phase transition. The strong peak of internal friction implies the large internal energy consumption during formation of different phases. Meanwhile, from the shape of the internal friction and the dependence of shear modulus on the frequency, it can be concluded that the $\text{GdBaCo}_2\text{O}_{5.005}$ system may undergo an intrinsic relaxation process below the charge ordering transition. Based on the results of neutron powder diffraction and electron diffraction, Mitchell *et al.* suggest there is no long-range charge ordering in the $\text{NdBaCo}_2\text{O}_5$ compound, or that charge ordering occurs possibly in only a small fraction of the sample.²³ In YBaCo_2O_5 ,

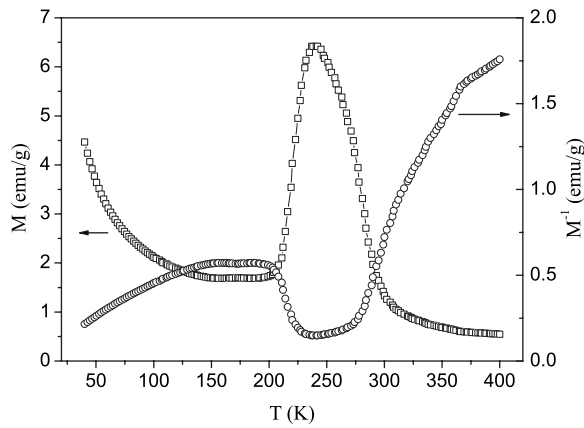


FIG. 3. The variation of the magnetization [$M(T)$] for $\text{GdBaCo}_2\text{O}_{5.499}$ in a field of 1 T as a function of the temperature (zero-field cooled and taken on heating).

the phase separation occurred simultaneously with the charge ordering transition was reported by Akahoshi and Ueda below T_{CO} .²⁴ There, they found that the crystal structure is the mixture consisting of orthorhombic phase and tetragonal phase at the low temperature ($T < T_{\text{CO}}$). These CO domains and the multiphase coexistence maybe exist in $\text{GdBaCo}_2\text{O}_{5.005}$, too. The relaxation process below T_{CO} may be associated with stress-induced motion of domain and/or phase boundaries. A similar relaxation mechanism was once used to explain the internal friction peak observed in $\text{Bi}_{0.4}\text{Ca}_{0.6}\text{MnO}_3$.²¹ In addition to the shear modulus softening and internal friction peak at about T_{CO} , we note an upturn in modulus curve at about 350 K. This anomaly may arise from the PM to AFM spin ordering which itself induces a small orthorhombic distortion of the unit cell. Resembling other lanthanide $R\text{BaCo}_2\text{O}_5$ compounds [$R = \text{Y},^3 \text{Ho},^{4,5} \text{Tb},^5 \text{Dy},^5$ and Nd (Ref. 23)], $\text{GdBaCo}_2\text{O}_{5.005}$ shows PM behavior at higher temperature, and when lowering temperature to T_N , the Co magnetic moments order in the form of so-called AFM G -type structure, for which each Co moment is AF coupled to its six nearest neighbors. The coupling between the lattice strain and magnetic moments is responsible for the anomaly of modulus at 350 K. This orthorhombic distortion is so small that the common x-ray powder diffraction experiment can hardly detect it out. As for no indications of the AFM state observed in the $M^{-1}(T)$ curve of $\text{GdBaCo}_2\text{O}_{5.005}$ may be ascribed to that the magnetization component coming from the Co ions is less important than that from the Gd ions.

As mentioned in the Introduction, all Co ions in $\text{GdBaCo}_2\text{O}_5$ ($\delta=0$) are located within square pyramids with a fivefold coordination. With increasing δ , the extra oxygen ions occupy the $[\text{GdO}_\delta]$ layers, providing an octahedral environment for a part of Co ions. Thus the different physical properties can be expected. Figure 3 shows the variation of the magnetization [$M(T)$] and its inverse as a function of the temperature measured after a zero-field cooling (ZFC) process. In contrast to $\text{GdBaCo}_2\text{O}_{5.005}$, $\text{GdBaCo}_2\text{O}_{5.499}$ exhibits a complicated magnetic feature. Below 300 K, the magnetization increases with decreasing temperature and develops

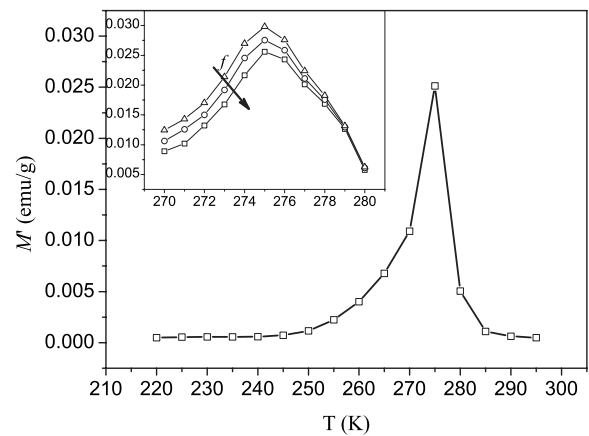


FIG. 4. Temperature dependence of the ac magnetic susceptibility for $\text{GdBaCo}_2\text{O}_{5.499}$ with a frequency of 1000 Hz. The inset shows the cusp in detail: (Δ) 5 Hz; (\circ) 100 Hz; (\square) 1000 Hz. All data were collected at an ac field of 30e on heating in the ZFC condition.

gradually an ferromagnetic (FM) ordering until 235 K, and then the magnetization steeply drops, indicating successive PM-FM-AFM transitions.^{1,2,6,11} These magnetic transitions are also shown by the ac susceptibility curve recorded in the ac-field of 3 Oe after ZFC (Fig. 4). A cusp at 275 K can be clearly seen from Fig. 4. The AFM ordering temperature from ac susceptibility curve is higher than that of magnetization curve. The frequency dependence of the cusp is shown in the inset of Fig. 4. Obviously, the peak is frequency-dependent below T_{cusp} , but does not exhibit a clear shift of T_{cusp} with f . Similar features were also observed by Martin *et al.* in $\text{EuBaCo}_2\text{O}_{5.4}$.¹ This behavior of $\text{GdBaCo}_2\text{O}_{5.499}$ is different from the typical spin glass materials,²⁵ indicating no spin glass state in $\text{GdBaCo}_2\text{O}_{5.499}$.

In order to obtain more information about these transitions, we carry out the measurements of internal friction and shear modulus on the samples with $\delta=0.499$ and 0.515. The results of the temperature dependence of the shear modulus and internal friction for $\text{GdBaCo}_2\text{O}_{5.499}$ were shown in Fig. 5. It can be seen that the shear modulus decreases slowly with increasing temperature at first. After passing through a minimum at about 243 K, the shear modulus begins to increase abruptly. Above 280 K, the modulus increases smoothly. Corresponding to the change of shear modulus, an asymmetric internal friction peak which has higher Q^{-1} at the low temperature side was also observed. Combined with the result of magnetic measurement as shown in Figs. 3 and 4, the changes of internal friction and shear modulus can be connected with the mechanical characterization of AFM-FM transition of the $\text{GdBaCo}_2\text{O}_{5.499}$ sample. However, it is possible that some ferromagnetic domains and/or phase boundaries between the AFM and FM phases may be formed during the AFM-FM transition, especially when the oxygen concentration with a distribution in the investigated ceramics samples, although we try to avoid it by annealing carefully them. The movements of domains and/or phase boundaries induced by the stress may result in the increasing of the Q^{-1} . The higher Q^{-1} at the low-temperature side of the internal

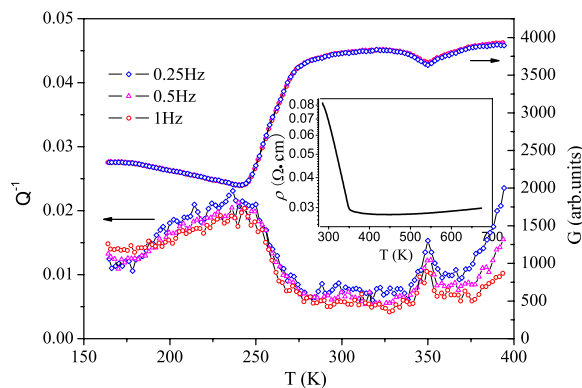


FIG. 5. (Color online) Temperature dependence of the shear modulus and internal friction of $\text{GdBaCo}_2\text{O}_{5.499}$ with various frequencies at a heating rate of 2 K/min. The inset shows the resistivity ρ as a function of temperature.

friction peak should be related to it. The relative change of shear modulus $(G_{\min} - G_{300\text{ K}})/G_{300\text{ K}}$, exceeds 40% during the AFM-FM transition. Such big change indicates the AFM-FM transition may be accompanied by a lattice distortion. However, this lattice distortion was not observed by Frontera *et al.* using synchrotron x-ray powder diffraction.⁹ As we have known, a large reduction of the modulus was often observed in the system of metallic glass such as $\text{Pd}_{77.5}\text{Cu}_6\text{Si}_{16.5}$.²⁶ In polycrystalline $\text{La}_{0.2}\text{Ca}_{0.8}\text{MnO}_3$, Li *et al.* observed also a large reduction of the modulus oxide, which was explained by the spin-glass behavior of the magnetic properties.²⁷ But the large reduction of the modulus in our $\text{GdBaCo}_2\text{O}_{5.499}$ sample is not associated with spin-glass behavior since we do not observe this behavior by the ac susceptibility measurement. Based on the detailed magnetization data of $\text{GdBaCo}_2\text{O}_{5+\delta}$, Roy *et al.*⁷ and Kim *et al.*⁸ suggested that the AFM-FM phase transition is not only simply understood as the spin-state transition, but the orbital ordering of the e_g electron should be considered. At low temperature Co^{3+} ions located in the octahedral site has a low spin state LS ($t_{2g}^6 e_g^0$), and with increase of temperature, the t_{2g} electrons of get thermally excited and an electron is transferred to e_g level resulting in a intermediate spin state IS ($t_{2g}^5 e_g^1$) which is Jahn-Teller active and may develop the orbital ordering. The coupling between the lattice strain and the orbital moment of e_g of Co^{3+} ion located in the octahedral site may result in the large increase of the shear modulus in $\text{GdBaCo}_2\text{O}_{5.499}$. As the temperature increases further, the PM phase appears and the shear modulus increases smoothly. Furthermore, we note in Ref. 11 that Taskin *et al.* reported the AFM ordering is sensitive to the oxygen stoichiometry: any deviation from $\delta=0.5$ will introduce Co^{2+} or Co^{4+} ions and should shift the AFM-FM phase transition to lower temperature. Our internal friction result of the samples with $\delta=0.515$ (seen in Fig. 6) is coincident with the above viewpoint. That is, the internal friction peak and large shear modulus softening corresponding to AFM-FM phase transition appeared at a lower temperature (about 180 K) compared to the samples with $\delta=0.499$.

In addition to the internal friction peak and large change of shear modulus G at low temperature, a small but clear inter-

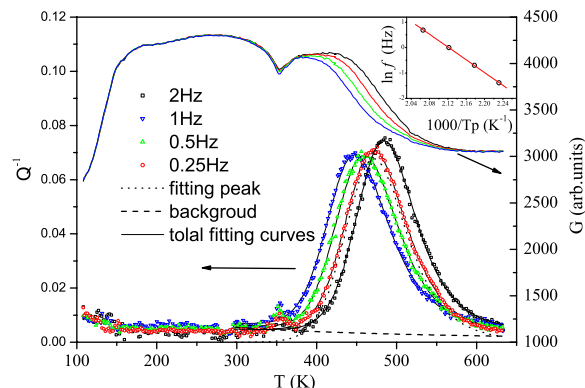


FIG. 6. (Color online) Temperature dependence of the shear modulus and internal friction of $\text{GdBaCo}_2\text{O}_{5.515}$ with various frequencies at a heating rate of 2 K/min. For curves of internal friction, the symbols are experimental data points and the solid lines are the total fitting results. The background of fitting is drawn as the dashed line. The inset shows $\ln f$ vs $1000/T_p$ curve.

nal friction peak is observed both from Figs. 5 and 6 around 350 K (the peak temperature T_p). This peak increases in height but hardly changes its positions as the frequency decreases, which are typical features of the phase transition. The corresponding modulus with a local minimum at T_p also characterizes the nature of phase transition. A rapid decrease in resistivity (on heating) is also observed at around 350 K (see inset of Fig. 5). The peak of the internal friction and resistivity anomaly coinciding at the transition temperature of metal-insulator reported by many researchers indicate that the internal friction peak here corresponds to metal-insulator transition. Combined with our result of magnetic susceptibility measurements, where a change in the paramagnetic susceptibility slope [$M^{-1}(T)$ curve in Fig. 3] at T_{MI} was observed, a strong relation between the metal-insulator transition and spin-state transition can be concluded. In Refs. 7 and 8, Roy *et al.* and Kim *et al.* have suggested the spin state transition only occur in octahedral sites, and corresponding to HS to IS upon cooling. The IS state of the Co^{3+} ions located in octahedral sites is Jahn-Teller active, but the HS state is inactive. Thus the change from Jahn-Teller active to Jahn-Teller inactive state results in the reduction of electron-lattice coupling and the delocalization of Co 3d electron. The reduction of electron-lattice coupling and the difference of the ionic radius of Co^{3+} ions under different spin states should bring a lattice change. This lattice change is well revealed by modulus change in internal friction measurement.

For $\text{GdBaCo}_2\text{O}_{5+\delta}$ ($\delta=0.499$ and 0.515), the internal friction Q^{-1} increase rapidly again as further increasing temperature above 375 K. A wide internal friction peak is observed at about 470 K for a vibration frequency of 1 Hz (see Fig. 6), accompanied by a corresponding decrease in the shear modulus. This peak shifts towards higher temperature with increasing frequency and exhibits typical relaxation characteristics, which could be well fitted by one Debye peak with distribution in relaxation time using a nonlinear fitting method,^{28,29} as shown in Fig. 6. The peak is slightly broader than a standard Debye relaxation peak. The distribution pa-

rameters for the internal friction peak are about 0.77 eV for β_O and $\beta_H \approx 0$, indicating that the internal friction has a distribution in the pre-exponential factor but not in the relaxation activation energy, where β_O and β_H are Gaussian distribution parameters of the pre-exponential factor and the activation energy of relaxation time, respectively.¹⁷

For a thermally activated relaxation process, the relation between the relaxation time τ and the absolute temperature T can be expressed as

$$\tau = \tau_0 \exp(E/kT), \quad (1)$$

where τ_0 is the pre-exponential factor, E is the activation energy of the relaxation process, and k is the Boltzmann constant. At the peak position the condition of $\omega\tau=1$ is fulfilled, where $\omega=2\pi f$ is the angular frequency. Substituting $\omega\tau=2\pi f\tau=1$ into Eq. (1), we have

$$\ln(2\pi f\tau_0) + E/kT_p = 0, \quad (2)$$

where T_p is the peak temperature. If one plot the $\ln f$ versus $1/T_p$, one could deduce the parameters of τ_0 and E for this internal friction peak. The so-called Arrhenius plot for the peak is shown in the inset of Fig. 6. From this figure, we obtained the relaxation parameters $E=1.08$ eV and $\tau_0=4.4 \times 10^{-13}$ s, which are the reasonable values for the migration of the oxygen ions in the oxides.^{18,29} Furthermore, our previous work has shown that this internal friction peak height decreases with decreasing the oxygen content δ ,³⁰ and it is not present in the samples with the oxygen content $\delta \approx 0$ (see Fig. 2 in this paper). These results suggest the peak was related to oxygen motion within the Gd-O planes. The GdBaCo₂O_{5+ δ} samples with the oxygen content $\delta = 0.499$ and 0.515 have a orthorhombic $Pmmm$ symmetry, thus the two crystallographically nonequivalent oxygen sites O3'(0,0,0.5) and O3(0,0.5,0.5) can be expected within the

Gd-O planes (See the inset of Fig. 1 in Ref. 10), and there should be a potential energy difference between them. The hopping of oxygen atoms induced by the stress between the two oxygen sites results in the relaxation internal friction peak. Similar oxygen relaxation behavior was widely reported in YBa₂Cu₃O_{7- δ} .^{18,31}

IV. CONCLUSION

The investigation of internal friction, shear modulus, electrical, and magnetic properties on GdBaCo₂O_{5+ δ} ($\delta=0.005$, 0.499 , and 0.515) indicates that there is a strong correlation among them. For GdBaCo₂O_{5.005}, the coupling between the charges and the lattice strain via the Jahn-Teller effect of HS-Co³⁺ ions located in square pyramidal sites leads to the internal friction peak and the anomaly of shear modulus at about T_{CO} . The anomaly of the shear modulus at around 350 K can be ascribed to a phase transition from PM phase to AFM phase, accompanying the lattice distortion.

For the case of δ near 0.5, such as 0.499 and 0.515, an internal friction peak together with the minimum of the shear modulus is observed around 350 K, and it is related to the metal-insulator transition driven possibly by a spin state transition of Co³⁺ ions from IS to HS state. The FM-AFM transition is accompanied by the obvious lattice softening. And a relaxation internal friction peak at higher temperature is also observed which originates from the oxygen hopping within the Gd-O planes.

ACKNOWLEDGMENT

This research was supported by the National Natural Science Foundation of China (Grant Nos. 10574123 and 50332040).

*wliu@ustc.edu.cn

¹C. Martin, A. Maignan, D. Pelloquin, N. Nguyen, and B. Raveau, *Appl. Phys. Lett.* **71**, 1421 (1997).

²A. Maignan, C. Martin, D. Pelloquin, N. Nguyen, and B. Raveau, *J. Solid State Chem.* **142**, 247 (1999).

³T. Vogt, P. M. Woodward, P. Karen, B. A. Hunter, P. Henning, and A. R. Moodenbaugh, *Phys. Rev. Lett.* **84**, 2969 (2000).

⁴E. Suard, F. Fauth, V. Caignaert, I. Mirebeau, and G. Baldinozzi, *Phys. Rev. B* **61**, R11871 (2000).

⁵F. Fauth, E. Suard, V. Caignaert, I. Mirebeau, B. Domengès, I. Mirebeau, and L. Keller, *Eur. Phys. J. B* **21**, 163 (2001).

⁶Y. Moritomo, T. Akimoto, M. Takeo, A. Machida, E. Nishibori, M. Takata, M. Sakata, K. Ohoyama, and A. Nakamura, *Phys. Rev. B* **61**, R13325 (2000).

⁷S. Roy, M. Khan, Y. Q. Guo, J. Craig, and N. Ali, *Phys. Rev. B* **65**, 064437 (2002).

⁸W. S. Kim, E. O. Chi, H. S. Choi, H. Hur, S. J. Oh, and H. C. Ri, *Solid State Commun.* **116**, 609 (2000).

⁹C. Frontera, J. L. Garcia-Munoz, A. Llobet, M. A. G. Aranda, J. Rodriguez-Carvajal, M. Respaud, J. M. Broto, B. Raguét, H.

Rakoto, and M. L. Goiran, *J. Am. Ceram. Soc.* **323-324**, 468 (2001).

¹⁰C. Frontera, J. L. García-Muñoz, A. Llobet, and M. A. G. Aranda, *Phys. Rev. B* **65**, 180405(R) (2002).

¹¹A. A. Taskin, A. N. Lavrov, and Yoichi Ando, *Phys. Rev. Lett.* **90**, 227201 (2003).

¹²C. Frontera, J. L. García-Muñoz, A. Llobet, A. Ll. Mañosa, and M. A. G. Arandac, *J. Solid State Chem.* **171**, 349 (2003).

¹³V. Caignaert, I. Mirebeau, F. Bourée, N. Nguyen, A. Ducouret, J. M. Greneche, and B. Raveau, *J. Solid State Chem.* **114**, 24 (1995).

¹⁴H. Wu, *Phys. Rev. B* **62**, R11953 (2000).

¹⁵J. Wang, W. Y. Zhang, and D. Y. Xing, *Phys. Rev. B* **66**, 052410 (2002).

¹⁶S. K. Kwon and B. I. Min, *Phys. Rev. B* **62**, R14637 (2000).

¹⁷A. S. Nowick and B. S. Berry, *Anelastic Relaxation in Crystalline Solids* (Academic Press, New York, 1972).

¹⁸X. M. Xie, T. G. Chen, and Z. L. Wu, *Phys. Rev. B* **40**, 4549 (1989).

¹⁹H. L. Zhang, X. S. Wu, C. S. Chen, and W. Liu, *Phys. Rev. B* **71**,

- 064422 (2005).
- ²⁰R. K. Zheng, A. N. Tang, Y. Yang, W. Wang, G. Li, X. G. Li, and H. C. Ku, *J. Appl. Phys.* **94**, 514 (2003).
- ²¹W. J. Lu, Y. P. Sun, B. C. Zhao, X. B. Zhu, and W. H. Song, *Phys. Rev. B* **73**, 214409 (2006).
- ²²*Colossal Magnetoresistive Oxides*, edited by Y. Tokura (Gordon & Breach Science Publishers, London, 1999).
- ²³J. F. Mitchell, Jonathan Burley, and Simine Short, *J. Appl. Phys.* **93**, 7364 (2003).
- ²⁴D. Akahoshi and Y. Ueda, *J. Solid State Chem.* **156**, 355 (2003).
- ²⁵J. A. Mydosh, *Spin Classes* (Taylor & Francis, London, 1993).
- ²⁶H. Y. Zhen and X. G. Li, *Phys. Status Solidi A* **99**, 115 (1987).
- ²⁷K. B. Li, X. J. Li, C. S. Liu, Z. G. Zhu, J. J. Du, D. L. Hou, X. F. Nie, J. S. Zhu, and Y. H. Zhang, *Phys. Rev. B* **56**, 13662 (1997).
- ²⁸L. X. Yuan and Q. F. Fang, *Acta Metall. Sin.* **34**, 1046 (1996).
- ²⁹X. P. Wang and Q. F. Fang, *J. Phys.: Condens. Matter* **13**, 1641 (2001).
- ³⁰W. Liu, Y. M. Zhang, X. S. Wu, and C. S. Chen, *Acta Phys. Sin.* **11**, 5996 (2006).
- ³¹Y. Mi, R. Schaller, S. Sathish, and W. Benoit, *Phys. Rev. B* **44**, 12575 (1991).